JOURNAL OF GEOPHYSICAL RESEARCH, VOL. 102, NO. B8, PAGES 18,071–18,090, AUGUST 10, 1997

Mapping of a magma reservoir beneath Nikko-Shirane volcano in northern Kanto, Japan, from travel time and seismogram shape anomalies

Shigeki Horiuchi,[1] Noriko Tsumura, and Akira Hasegawa

Research Center for Prediction of Earthquakes and Volcanic Eruptions, Faculty of Science
Tohoku University, Sendai, Japan

Abstract. Since ray paths of direct *P* and *S* waves are largely distorted in a magma body, a seismic shadow zone is created. However, scattered or diffracted waves with very small amplitudes can arrive in the shadow zone because their ray paths are different from those of the direct waves. They become the first arrival in the shadow zone. More than 100 seismologists from many institutions in Japan joined together to perform an intensified seismic study in the Nikko-Ashio area, northern Kanto, Japan. It was suggested that there is a magma body beneath Mount Nikko-Shirane, an active volcano, that causes a seismic shadow zone, because *P* waves recorded by the joint observation are anomalously attenuated in cases when they propagate through a zone beneath the eastern part of the volcano. We developed a new method to estimate the shape of the anomalous attenuation zone by proposing the use of a new parameter, the energy ratio between direct*P* or *S* waves and their coda waves, to discriminate whether or not each observation station is located inside or outside the shadow zone. We estimated the shape of the anomalous attenuation zone by dividing the study area into blocks with dimensions of 2 km x 2 km x 1 km and using the energy ratio data of *P* waves for local events. The obtained result shows the existence of an anomalous attenuation zone in the area east of Nikko-Shirane volcano with a diameter of about 10 km at depths greater than 3 km. It was also found from plots of deep event seismograms recorded by the same observation that travel times are delayed by about 0.7 s for ray paths crossing the anomalous attenuation zone obtained by the energy ratio data. This value requires the *P* wave velocity in the anomalous zone to be less than that of the surrounding crustal material by at least about 30%, suggesting the existence of a huge magma reservoir in this area.

Introduction

The northeastern Japan arc is a typical subduction zone in which the volcanic chain extends along the middle of the arc nearly parallel to the trench axis. *Hasemi et al.* [1984], *Obara et al.* [1986], and *Zhao et al.* [1992, 1994] found seismic low-velocity zones beneath active volcanoes in this arc by inverting travel time data obtained by the seismograph network of Tohoku University. They pointed out that these low-velocity zones are distributed in the crust beneath volcanic areas and become deeper toward the west in the mantle wedge.

The Nikko-Ashio area in northern Kanto is one such volcanic area with low-velocity zones. Using data from a temporary seismic experiment in this area, *Ogino* [1974] and *Mizoue et al.* [1982] found remarkable later phases in seismograms from shallow earthquakes. These were interpreted as a reflected *S*- to -*S* wave (*S*x*S*) and a reflected *S* to *P* converted wave (*S*x*P*) from the upper surface of a very low rigidity zone, such as a magma body in the middle crust. *Horiuchi et al.* [1988] and *Matsumoto and Hasegawa* [1996] also made seismic observations and pointed out that the midcrustal reflector is at least 10 km x 6 km in areal extent, and it becomes shallow toward an active volcano, Mount Nikko-Shirane. Two earthquake swarm areas are located close to and above this reflector.

Similar midcrustal reflectors have been found in several areas of Japan, such as in the earthquake swarm area of Matsushiro, Nagano Prefecture [*Nishiwaki et al.*, 1989], in the aftershock area of the 1984 Western Nagano Prefecture earthquake, which occurred near Ontake volcano [*Mizoue and Ishiketa*, 1988; *Inamori et al.*, 1992], near Mount Moriyoshi, Akita Prefecture [*Hori and Hasegawa*, 1991], and near Azuma volcano, Fukushima Prefecture [*Hasegawa et al.*, 1991]. These reflectors have the same features as those found at the Rio Grande Rift, New Mexico

[1] Now at Department of Earth Science, Faculty of Science, Chiba University, Chiba, Japan.

Paper number 97JB00974.
0148-0227/97/97JB-00974$09.00

[*Sanford et al.*, 1973]. Detailed studies on the crustal structure in this last area have been made by using reflection phases from the crust [*Brown et al.* , 1980; *Ake and Sanford*, 1988]. *Ake and Sanford* [1988] analyzed reflection phases of *PxP* and *SxS* and estimated the internal structure of the reflector body. They pointed out that the thickness of the reflector body found at the Rio Grande Rift is very small, <150 m.

A laboratory experiment by *Murase and Suzuki* [1966] shows the *P* wave velocity of a molten rock to be 2.5 - 3 km/s, which is about 50% of that for a normal rock. Yamamoto *et al.* (1981) calculated a theoretical *P* wave velocity for partially melted media. They pointed out that 10 and 20% of melting are enough to decrease *P* wave velocity by 30 and 50%, respectively.

If there exists a spherical magma body whose *P* wave velocity and diameter are 3 km/s and 10 km, respectively, in a homogeneous medium, the maximum travel time delay of the *P* wave propagating through it is expected to be around 1 s. However, the travel time of diffracted or scattered waves off the spherical body may be shorter than that of the direct *P* wave through the body. In a case when the observation station is located at a point 10 km away from the center of the magma body, the travel time delay of the diffracted wave is only 0.05 s. Therefore it is rather difficult to determine the precise shape and value of the velocity perturbation from a simple analysis using only first arrival time data.

Horiuchi et al. [1990] estimated a theoretical amplitude of the short period diffracted wave with frequencies ranging from 8 to 10 Hz by using a structural model of a spherical cavity with a diameter of 5 km located at a point 10 km away from the receiver. They pointed out that the amplitude of the diffracted wave near the center of the shadow zone is 1/3 to 1/5 of the direct wave in the homogeneous medium. This means that the first arrival is the diffracted or scattered wave with very small amplitude. Therefore it is rather difficult to determine the precise shape and value of the velocity perturbation from a simple analysis using only first arrival time data.

Many authors [e.g., *Ono et al.*, 1978; *Catchings*, 1988; *Lees and Crosson*, 1989; *Dawson et al.*, 1990; *Chiarabba et al.*, 1995; *Romero et al.*, 1993] have estimated three-dimensional seismic velocity structures beneath active volcanoes by inverting travel time data obtained from seismic networks set up around volcanoes. Though these results show the existence of anomalously low-velocity zones beneath volcanoes, the inferred seismic velocities are lower by only several percent than that for the surrounding region. It seems that a very clear image of magma bodies beneath volcanoes cannot be obtained by the ordinary tomographic inversion using only travel times of first arrivals.

Horiuchi et al. [1990] showed that an anomalous attenuation zone with a diameter of about 5 km exists beneath the eastern region of Bandai volcano, Fukushima Prefecture, which erupted 100 years ago. They used a large number of seismograms recorded at two stations near the volcano from local events that occurred around it. Plotting the seismograms as a function of backazimuths measured from the station to the epicenter, they showed that amplitudes of the initial parts of *P* and *S* waves passing through the eastern part of the volcano are very small compared with their coda waves, whose ray paths are considered to be different from those of the direct *P* and *S* waves. This suggested that the amplitude of the short period direct *P* and *S* waves decreases drastically by travel through the anomalous attenuation zone.

In 1993, high resolution seismic experiment was carried out in and around the Nikko-Ashio area to study the detailed crustal structure beneath the area and its relation to seismic and volcanic activity [*Hasegawa*, 1994] with installation of 38 telemetered stations and 200 event recorders along two 7 km long profiles. More than 100 people from many institutions in Japan joined this experiment (Joint Seismic Observation1993; JSO'93). An active volcano, Mount Nikko-Shirane, and Quaternary volcanoes, Mount Nantai, Mount Sukai, and Mount Nyoho-Akanagi, are in the area covered by the intensified seismic network. In this study, we developed a new method to determine the shape and location of anomalous attenuation zones. The method uses energy ratios between *P* or *S* waves and their coda waves. We present a detailed crustal structure beneath the Nikko-Ashio area based on the data obtained by the JSO'93.

Joint Seismic Observation 1993

As shown in Figure 1, we set up a joint seismograph network with a dimension of about 60 km x 60 km in the Nikko-Ashio area. The observation period was $2\frac{1}{2}$ months, from the middle of September to the end of November 1993. Thirty-eight telemetered stations were installed during the first 2 months. Then the number of stations was decreased to 11. All stations were equipped with three-component seismometers. The natural frequency of the seismometers was 1 Hz for 25 stations and 2 Hz for the remaining stations. In addition to the telemetered stations, 200 array stations equipped with remote controlled event recorders were set up along two profiles of about 7 km long with intervals of about 70m [*Group for the 1993 Joint Seismic Observation(JSO'93)*, 1994]. The data from the array stations are not discussed in this study.

Waveform data from telemetered stations were collected at the observation center of the network and were processed by an automatic system developed by *Horiuchi et al.* [1992]. This system uses a UNIX computer,

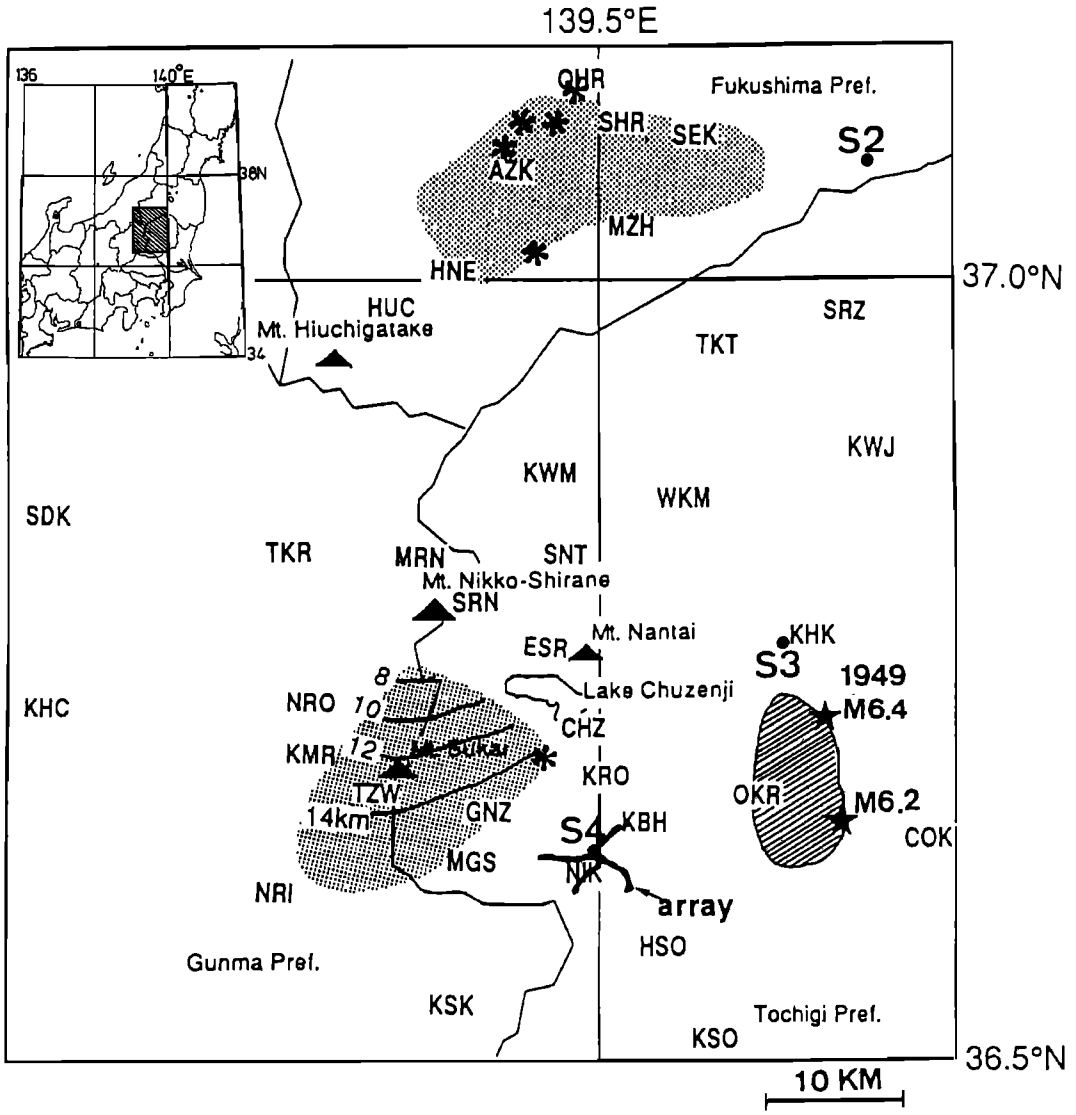

Figure 1. A map showing the temporary seismic observation network by JSO'93 in the Nikko-Ashio area [after *Hasegawa*, 1994]. The code letters are the location of telemetered stations. Two hundred array stations were set along two 7 km long observation lines shown as solid lines. S2 to S4 were the locations of shot points for the explosion experiment. Shaded zones in the northern and southern parts indicate the locations of midcrustal reflectors detected by *Iwase et al.* [1989] and *Matsumoto and Hasegawa* [1996], respectively. The contours plotted at the south of Mount Nikko-Shirane show the depth of the reflectors determined by *Matsumoto and Hasegawa* [1996]. Asterisks show the locations of low-frequency microearthquakes located by *Tsukada and Urabe* [private communication, 1994]. The hachured zone in the eastern part indicates an aftershock area of the *M*6.4 Imaichi earthquake in 1949. The stars within the hachured zone show the locations of main events of *M*6.4 and 6.2.

which automatically detects, locates, and records seismic events. Waveform data for about 4000 local and regional events were recorded during the entire observation period. Figure 2 shows the hypocenter distribution of 1428 local events located by the automatic system by using waveform data stored on an optical disk. These hypocenters have more than 8 picked *P* wave arrival times and most of them have standard errors in horizontal and vertical directions less than 400 m. It is clear that the depths of the deepest events shallow toward the north. Beneath Nikko-Shirane volcano, there are no events at depths greater than about 2 km. The accuracy of hypocenter locations by the automatic system appears to be very high, since the scatter of hypocenters in each cluster, even in the depth direction, is small.

Ito et al. [1995] pointed out that the seismic activity

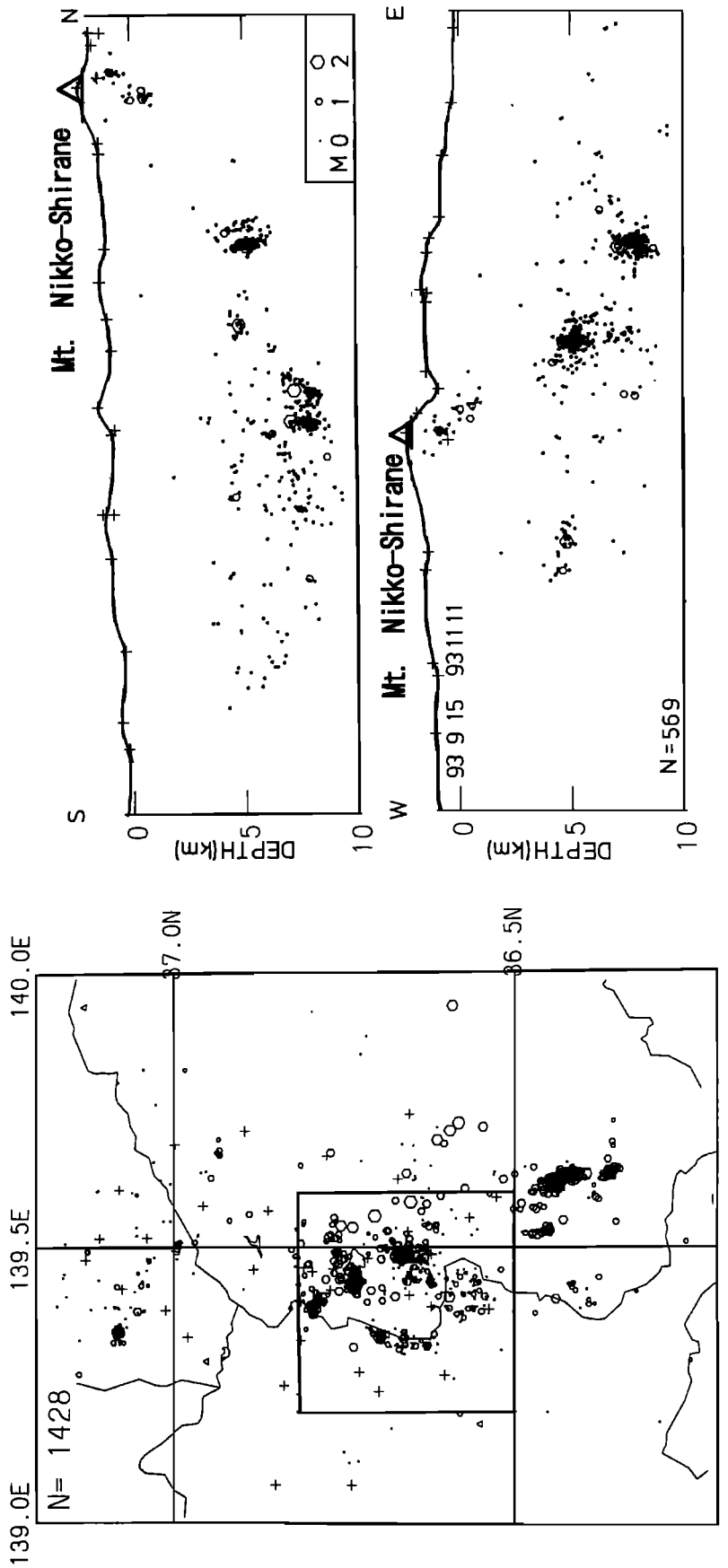

Figure 2. Hypocenter distribution obtained by the automatic event detection and location system [*Horiuchi et al.*, 1992] during the observation period of JSO'93. (left) Map with crosses showing the locations of telemetered stations. (right) N-S and E-W vertical cross sections in the region enclosed by the rectangle in the map.

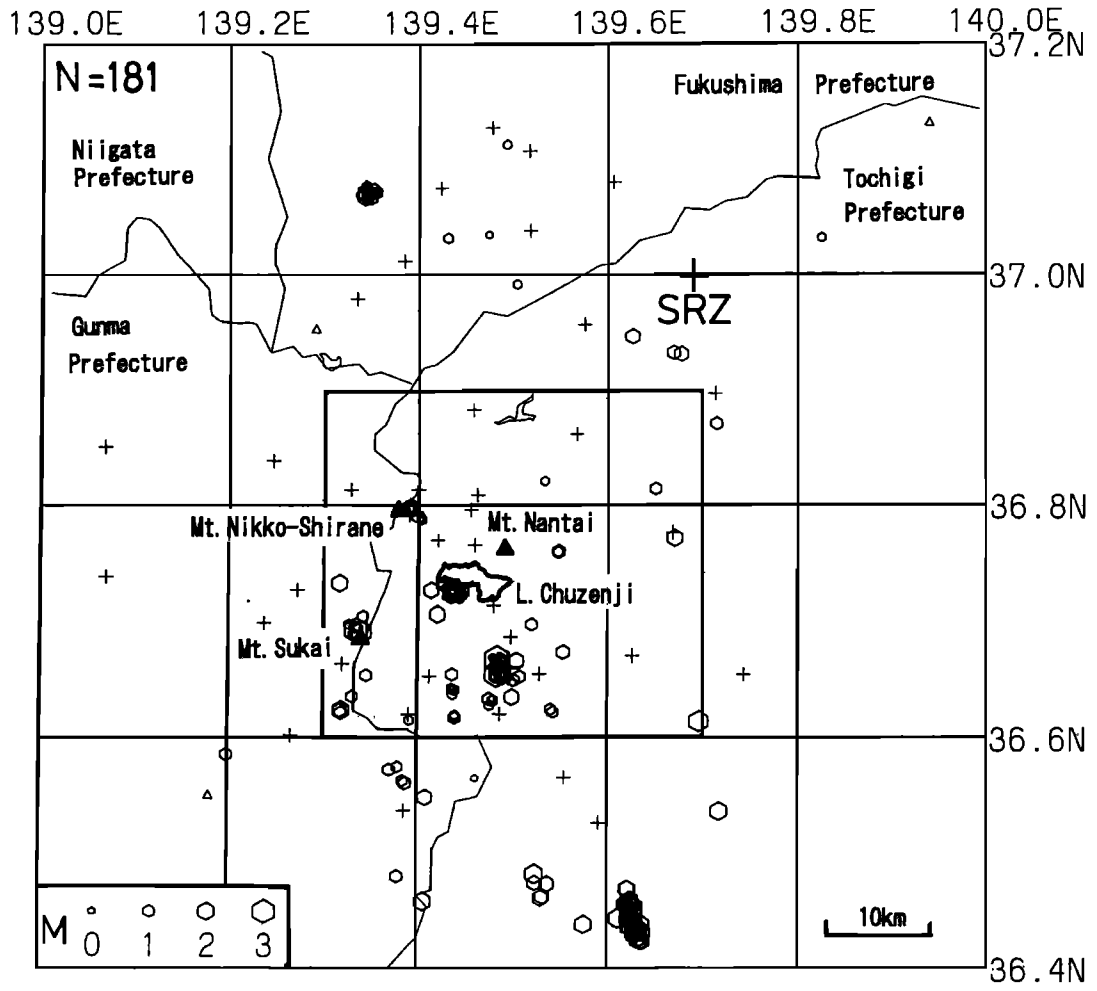

Figure 3. Epicenter distribution of relatively large events used in the present analysis. Crosses show the location of telemetered stations. The square shows the study area in Figures 9, 10, and 11.

beneath Nikko-Shirane volcano has increased since October 1994. They showed that there have been periods during which many small earthquakes occurred almost continuously. Seismograms from these events showed volcanic tremor, which is frequently observed before volcanic eruptions at many volcanoes.

Figure 3 shows an epicenter distribution of 195 relatively large events, for which more than 20 arrival times are picked by the automatic processing system. The magnitudes of most of these events are larger than 1.7. In the present analysis, we used waveform data for these events. Since it is very important to determine precise hypocenters for the accurate imaging of anomalous regions, we relocated hypocenters by using an inversion technique developed by *Horiuchi et al.* [1982], which determines station corrections and hypocenters for all events simultaneously. This method expresses the hypocenter parameters of each event with function of station corrections, and calculates matrix elements for the normal equations including unknown parameters of only station corrections by eliminating hypocenter parameters. A value of the root mean square of residuals before the inversion was 0.093 s and it became 0.065 s after the inversion. Although we used arrival time data picked by the automatic processing system, the root mean square residual after the inversion was very small.

Imaging of an Anomalous Zone

As schematically illustrated in Figure 4, let us consider that an earthquake occurs near a volcano beneath which there is a magma body characterized by low seismic velocities. The *P* and *S* waves emitted from the source will undergo large deflections at the surface of the magma body. If the shape of the magma body is not a thin rectangle, the deflected seismic waves will propagate to somewhere far from the volcano. Thus a shadow zone for direct *P* and *S* will be formed in the area of the upward extension of ray paths crossing the magma body. However, scattered waves, whose amplitude are much smaller than that of the direct *P* or *S* wave, will

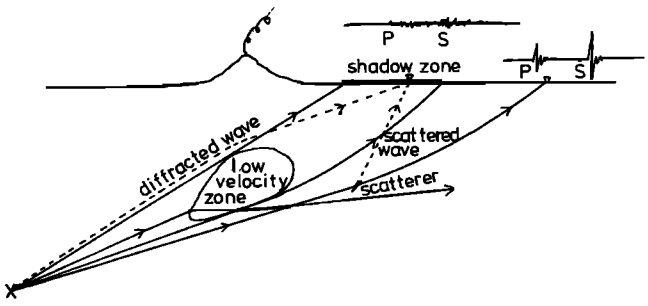

Figure 4. A schematic vertical cross section showing the characteristic features of seismograms inside and outside the shadow zone. A seismic shadow zone, where the direct *P* and *S* waves cannot arrive, is made by the existence of a magma body because the ray path is curved largely at its surface. Characteristic seismograms inside and outside of the shadow zone are schematically shown at the top.

be observed even in the shadow zone, since the crust is very heterogeneous.

A seismogram observed at a station in the shadow zone may have ambiguous *P* and *S* waves, as schematically shown at the top of Figure 4. On the contrary, clear direct *P* and *S* waves can be observed at stations outside the shadow zone. If we can distinguish between observation stations in and outside the shadow zone from the shape of their seismograms, we may image a very detailed structure of the anomalous zone by using many data for various ray paths.

Figures 5a, 5b, and 5c show three examples of seismograms demonstrating a large change in the shape of observed seismograms caused by the difference of ray paths. We plotted observed seismograms for events recorded at SRZ(Figure 5a), MZH(Figure 5b), and KHC(Figure 5c) stations, which are shown in Figure 2.

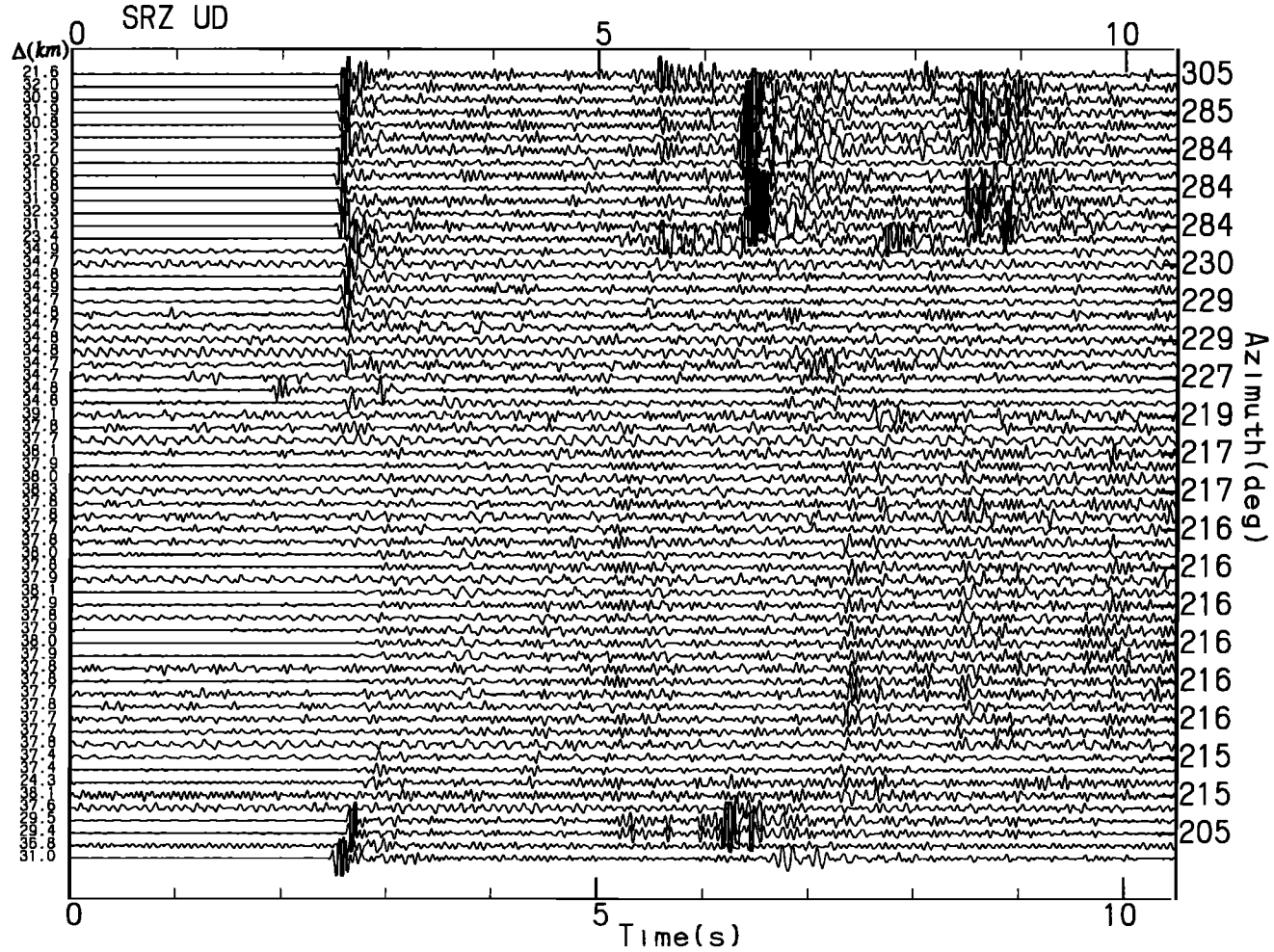

Figure 5a. Plot of vertical component seismograms for relatively large local events recorded at SRZ station that demonstrates the existence of an anomalous *P* wave attenuation zone to the east or south of Nikko-Shirane volcano. Seismograms are plotted in the order of backazimuths, angles from this station to hypocenters measured clockwise from north. These are seismograms for events shown in Figure 3 with epicentral distances larger than 20 km and less than 40 km. Time axes are shifted so that theoretical *P* wave arrival times become 3 s. Small numbers at the left side indicate epicentral distances.

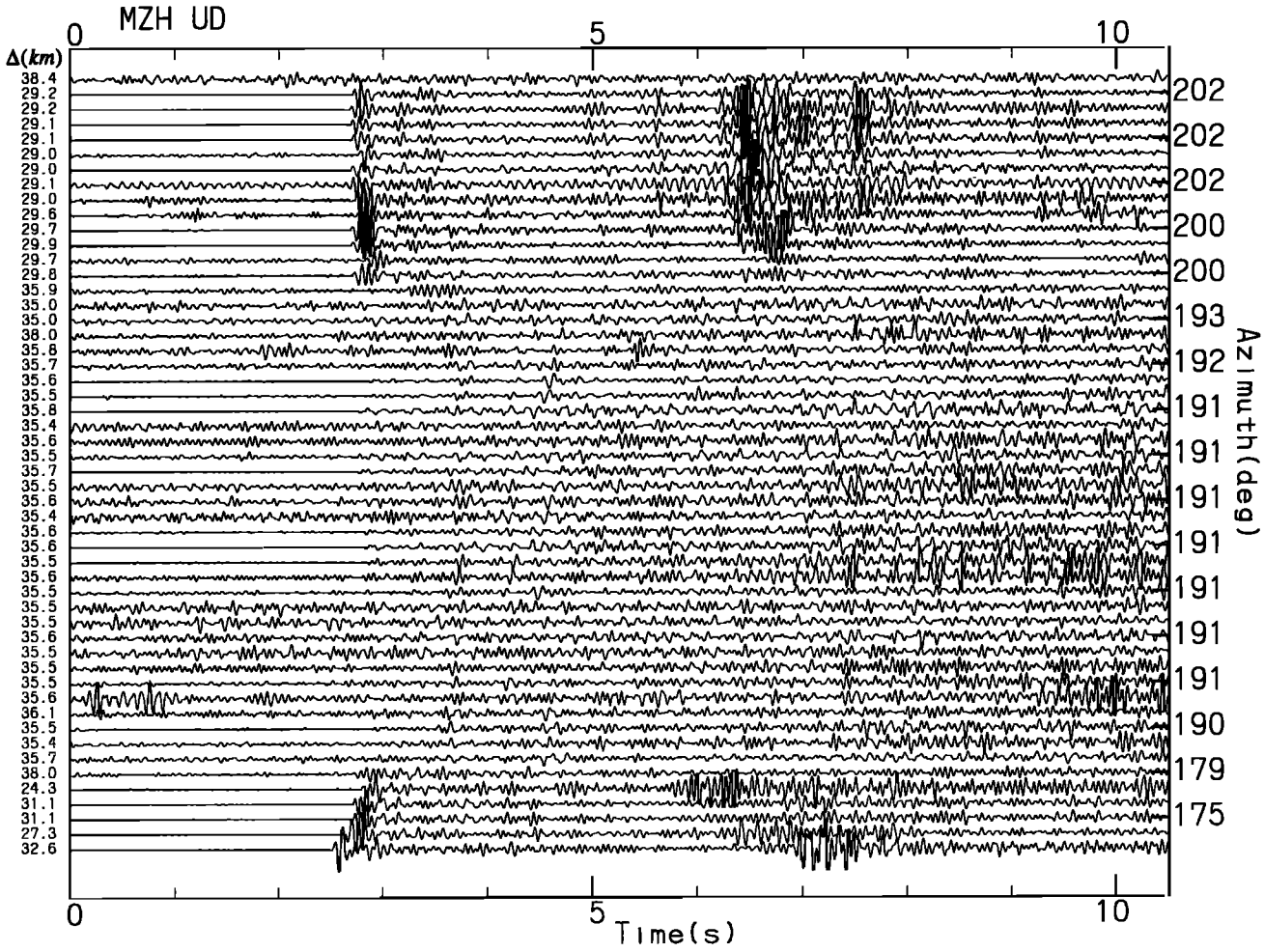

Figure 5b. Plot of vertical component seismograms for relatively large local events recorded at MZH station. Small numbers at the left side indicate epicentral distances.

Seismograms with epicentral distances ranging from 20 km to 40 km are exhibited in the order of backazimuths of epicenter locations measured clockwise from the stations. The time axis is shifted in each seismogram so that the theoretical arrival time of the direct *P* wave becomes 3 s. We scale the amplification according to the maximum amplitude of the *P* coda waves in a 0.5 s time window 2 s after the theoretical *P* wave arrival. We plotted the waveform data for the large events, having more than 20 *P* arrival time readings by the automatic system.

Stations SRZ and MZH are located at the northern part of the temporary seismic network. The backazimuths to the direction of Nikko-Shirane volcano from SRZ and MZH stations are 230° and 206°, respectively. All records of *P* and *S* waves propagating through the area south or east of Nikko-Shirane volcano undergo important attenuation; this is not true for ray paths with backazimuth larger than 230° or less than 216° in the case of SRZ station and backazimuth larger than 200° or less than 180° for MZH station.

Station KHC is located at the western end of the network. Most of *P* and *S* waves to this station propagate through the region above the distinct seismic reflector (Figure 1) found by *Horiuchi et al.* [1988] and *Matsumoto and Hasegawa* [1996]. However, as can be seen in Figure 5c, almost all *P* and *S* waves are very clear. This suggests that the obscurity in the observed seismograms in Figures 5a and 5b is not caused by the weak seismic signals generated by small size events. It is also difficult to consider that the obscurity is caused by the orientation of focal mechanisms since there are more than 20° of azimuthial differences between ray paths to SRZ and MZH stations from events occurring in the area south of Lake Chuzenji (Figure 3). This suggests the existence of an anomalous attenuation zone in the southern or eastern part of Nikko-Shirane volcano.

As shown in Figures 4 and 5, the amplitude of coda waves is not changed much by the existence of a low-velocity zone, because their ray paths are different from those of the direct *P* and *S* waves. This

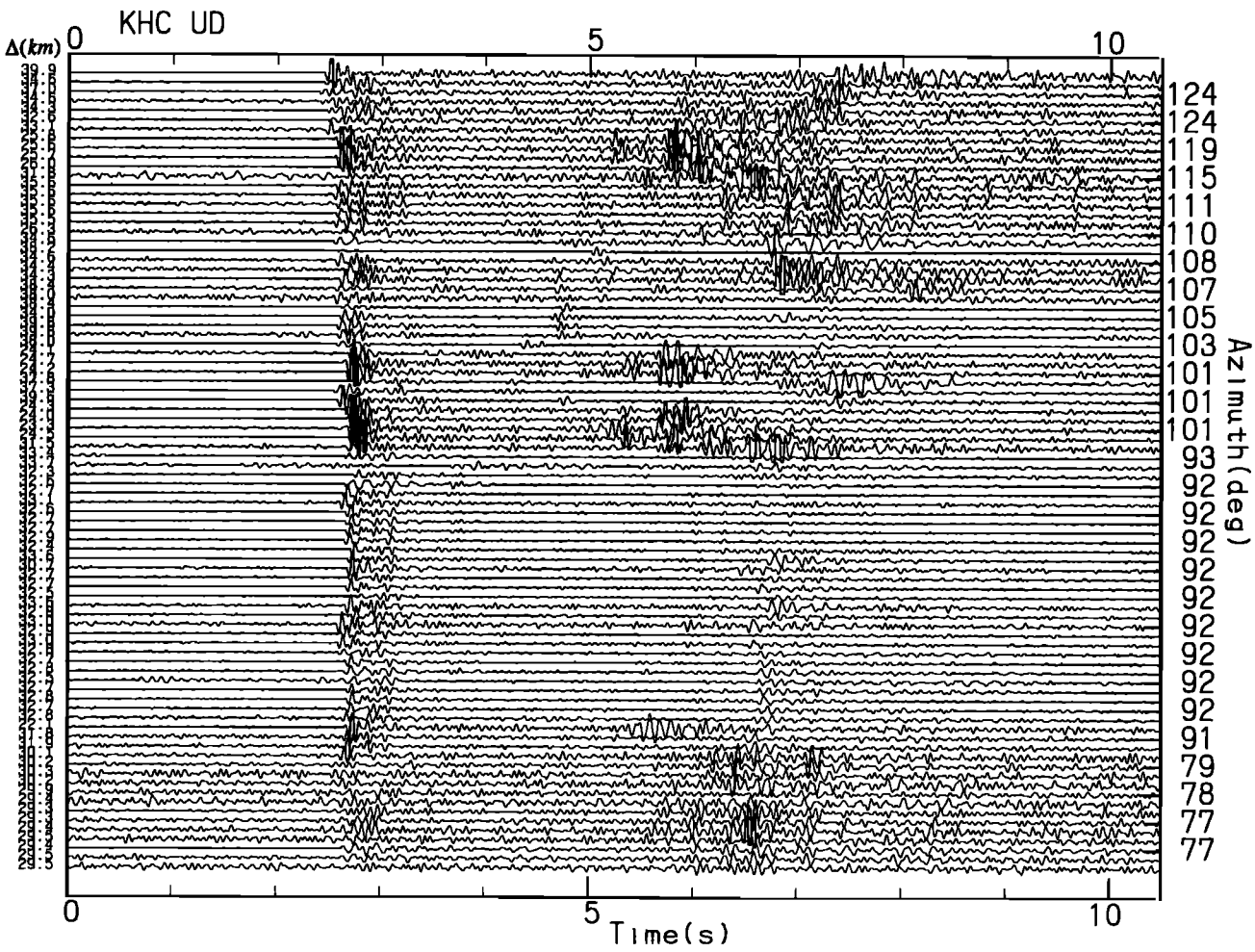

Figure 5c. Plot of vertical component seismograms for relatively large local events recorded at KHC station. Small numbers at the left side indicate epicentral distances.

consideration suggests that the energy ratio between the direct P or S wave and its coda wave may be a good indicator for discriminating whether or not an anomalous zone exists along the ray path of the direct wave. Thus, we define the ratio of the seismic energy as

$$r = E_p/E_{\text{total}} \quad (1)$$

where E_p and E_{total} are observed seismic energy for the initial part of the direct P wave and that for both the P and its coda waves, respectively. We calculate E_p and E_{total} by summing squares of velocity amplitudes in each time window. In the present study, the time windows for E_p and E_{total} are taken as 20% and 80% of S-P time starting from the direct P arrival time, respectively. In the case of the S wave, time windows are taken as the same duration as that of the P wave but starting from the direct S wave arrival time. We presume that this parameter is a good indicator for expressing clearness of the seismograms since it is small for obscure waveforms and is large for seismograms having a clear direct P wave.

Values of the energy ratio thus calculated are plotted on an E-W vertical section crossing the summit of Nikko-Shirane volcano (Figure 6). Figures 6a and 6b show the result for P and S waves, respectively. Large and small circles indicate rays having an energy ratio less than 0.25 and 0.5, respectively. Large crosses show values between 0.5 and 0.75, and small crosses show larger than 0.75 values. Symbols are plotted at the intersection point of each ray on the vertical section. We removed ray paths crossing the vertical section slantwise with angles between ray paths and the direction normal to the vertical section larger than 70° . The calculated energy ratios are very small for ray paths propagating through the eastern part of Nikko-Shirane volcano at depths greater than about 4 km. The results for P and S waves are similar to each other.

The frequency distribution of energy ratios is shown in Figure 7. About two thirds of the seismograms have energy ratios larger than 0.4. There are two peaks at values around 0.2 and 0.6-0.7. Here let us

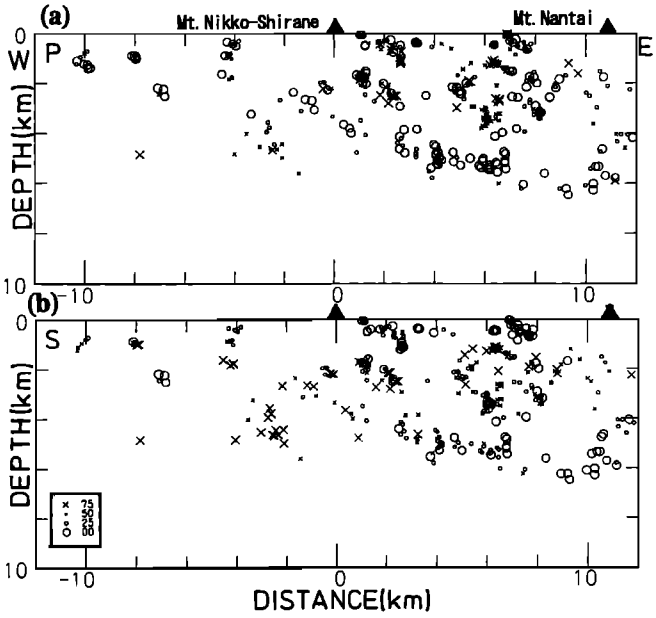

Figure 6. E-W vertical cross sections of intersection points of ray paths for (a) *P* waves and (b) *S* waves. Circles and crosses indicate ray paths with energy ratios less than and larger than 0.5, respectively. The origin of the horizontal axis is taken to be the summit of Nikko-Shirane volcano. Ray paths crossing the vertical section slantwise with angles less than 20° are removed.

assume that ray paths with energy ratios less than 0.4 are those which passed through anomalous zones and ray paths with energy ratios larger than 0.6 are those not passing through anomalous zones. A ray with energy ratio less than 0.4 is called a "hot" ray, and one within a ratio larger than 0.6 is called a "cold" ray. We assume that an observation station for a hot ray is in the shadow zone and outside for a cold ray.

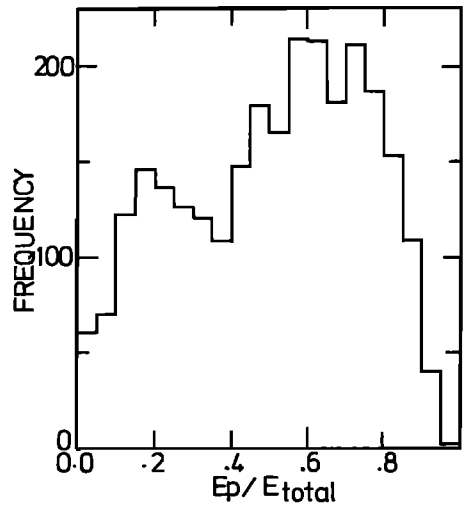

Figure 7. Frequency distribution of the energy ratio between *P* wave and its coda wave.

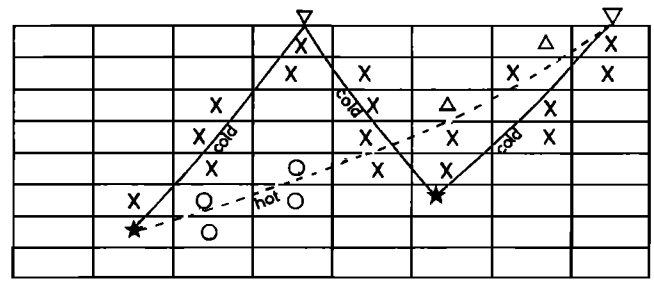

Figure 8. A schematic vertical cross section showing how to image anomalous blocks by the use of energy ratios. First, all blocks along a hot ray (dashed line) are considered to be hot blocks (circles). Then, blocks along a cold ray (solid line) are put to be cold blocks (crosses) even if they have many hot ray paths. Triangles show uncertain blocks which have no hot rays except crossing a cold blocks below.

Although we know the anomalous zone lies somewhere along a hot ray path, it is still difficult to determine where along the ray path the anomalous zone actually lies. Next, we divide the study area into small blocks so as to image the geometry of the anomalous attenuation zone. We calculate a hit number for each block which is the number of hot and cold rays passing through the block. As schematically shown in Figure 8, we first assume that all blocks along a cold ray have an ordinary seismic velocity.

We took the energy ratio, E_p/E_{total} as an indicator to define clearness of seismograms. Since we did not take into account the effects of the focal mechanism, Q structure, and earthquake size in the calculation of the energy ratio, it may be difficult to consider that there is always an anomalous zone somewhere along the hot ray path. Therefore we assume that a block having cold rays more than a small critical number, N_C, has a normal velocity, even if it has a large number of hot rays. We call this block a "cold" block. We further assume that a block has an anomalously low velocity, if its hit count for cold rays is less than N_C but hit count for hot rays is more than a small critical number, N_h,. We call it a "hot" block.

It is necessary to assume N_C and N_h for the actual calculation. We use energy ratio data for 2685 rays from 112 events which occurred in the study area. The block sizes are 2 km, 2 km, and 1 km in the N-S, E-W and vertical directions, respectively. The total number of blocks is 35 x 25 x 8 = 7000. The numbers of blocks having hit counts for hot rays more than 1, 2, 3, 4, and 5 are 2350, 1881, 1548, 1328, and 1139, respectively. The numbers of blocks having hit counts for cold rays more than 1, 2, 3, 4, and 5 are 2297, 1708, 1426, 1205, and 1062, respectively. Since the energy ratio data are limited, it is

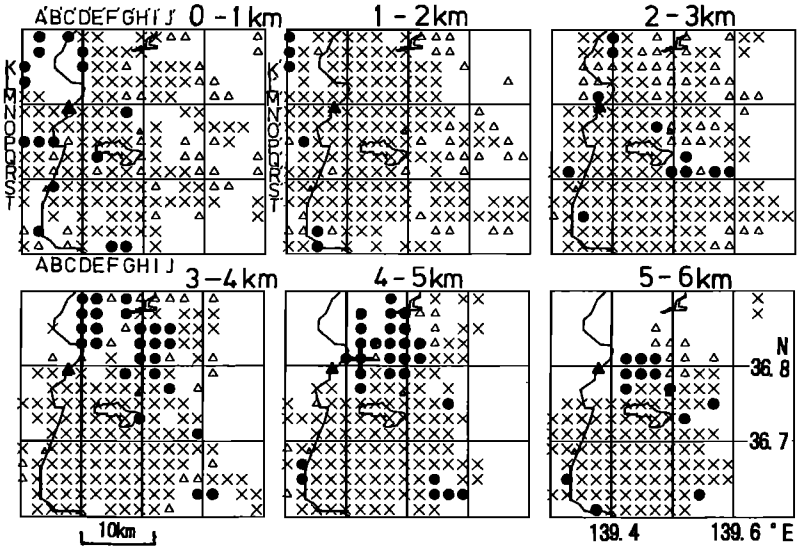

Figure 9. Map view showing distributions of hot(solid circles), cold(crosses), and uncertain(triangles) blocks at depth intervals of 1 km estimated from values of the energy ratio for *P* waves. Letters A-A' through J-J' and K-K' through T-T' indicate locations of N-S and W-E vertical cross sections shown in Figures 10 and 11, respectively. The plus in the result from 4 to 5 km shows the origin point to calculate distance of ray paths in Figures 14, 15, and 16. See text for the explanation of hot, cold, and uncertain blocks.

difficult to assume Nc and N_h to be a large number. We assumed both N_h and N_C to be 3 in this study. We will discuss this assumption later.

The spatial distribution of hot and cold blocks thus obtained is shown in Figures 9-11. If there are enough data from a large number of events distributed uniformly in space, the hit count for hot or cold rays becomes larger than a some critical value at most of the blocks. In this case, we can distinguish all cold blocks from hot blocks. However, as is clear from Figure 3, most events occur in the area south of Lake Chuzenji. We may not be able to distinguish some of the cold blocks from hot blocks because of insufficient ray coverage.

Let us consider the case that there are cold blocks in the middle of a hot ray path. If the shape of the anomalous zone is simple, there may be hot blocks along the hot ray path either in the deeper side or in the shallower side of the cold blocks. After determining the distribution of hot and cold blocks, we recalculated the hit counts of hot rays by neglecting ray paths shallower than mapped cold blocks, blocks with triangles in Figure 8. Open triangles in Figures 9-11 show blocks whose recalculated hit counts for hot rays is less than N_h. We call these blocks uncertain blocks.

Figure 9 shows distribution of the hot and cold blocks. Hot blocks are located in the area north of Lake Chuzenji and east of Nikko-Shirane volcano at depths greater than 3 km. The present result also shows that there are no anomalous zones above the midcrustal seismic reflector found by *Horiuchi et al.* [1988] and *Matsumoto and Hasegawa* [1996]. This reflector is located to the southeast of Nikko-Shirane volcano at depths greater than about 8 km and it becomes shallower toward Nikko-Shirane volcano with a dip angle of about 40° (Figure 1).

Figures 10 and 11 are N-S and E-W vertical cross sections showing the locations of hot and cold blocks. Solid lines indicate the location of the midcrustal seismic reflector estimated by *Matsumoto and Hasegawa* [1996]. Hot blocks are distributed on the upper and the northern extension of the seismic reflector (Figure 10). Since only shallow events are used in the present analysis, we could not estimate the lower boundary of the anomalous zone.

Since we assume both N_C and N_h to be 3, we checked how well the obtained hot and cold block model fit the energy ratio data. First, we calculate the number of hot blocks along the ray path of each seismogram. Next, we classify values of energy ratio for ray paths according to the number of hot blocks along them. Then we compute average values of energy ratios according to these numbers. As can be seen from Figure 12, the average value without hot blocks is 0.59. It decreases to 0.42 for seismograms relative to rays passing through only one hot block. The ratio gradually decrees to 0.2 when the number of hot blocks is 14.

As described before, a shadow zone is formed by the existence of a magma body, and the scattered or diffracted

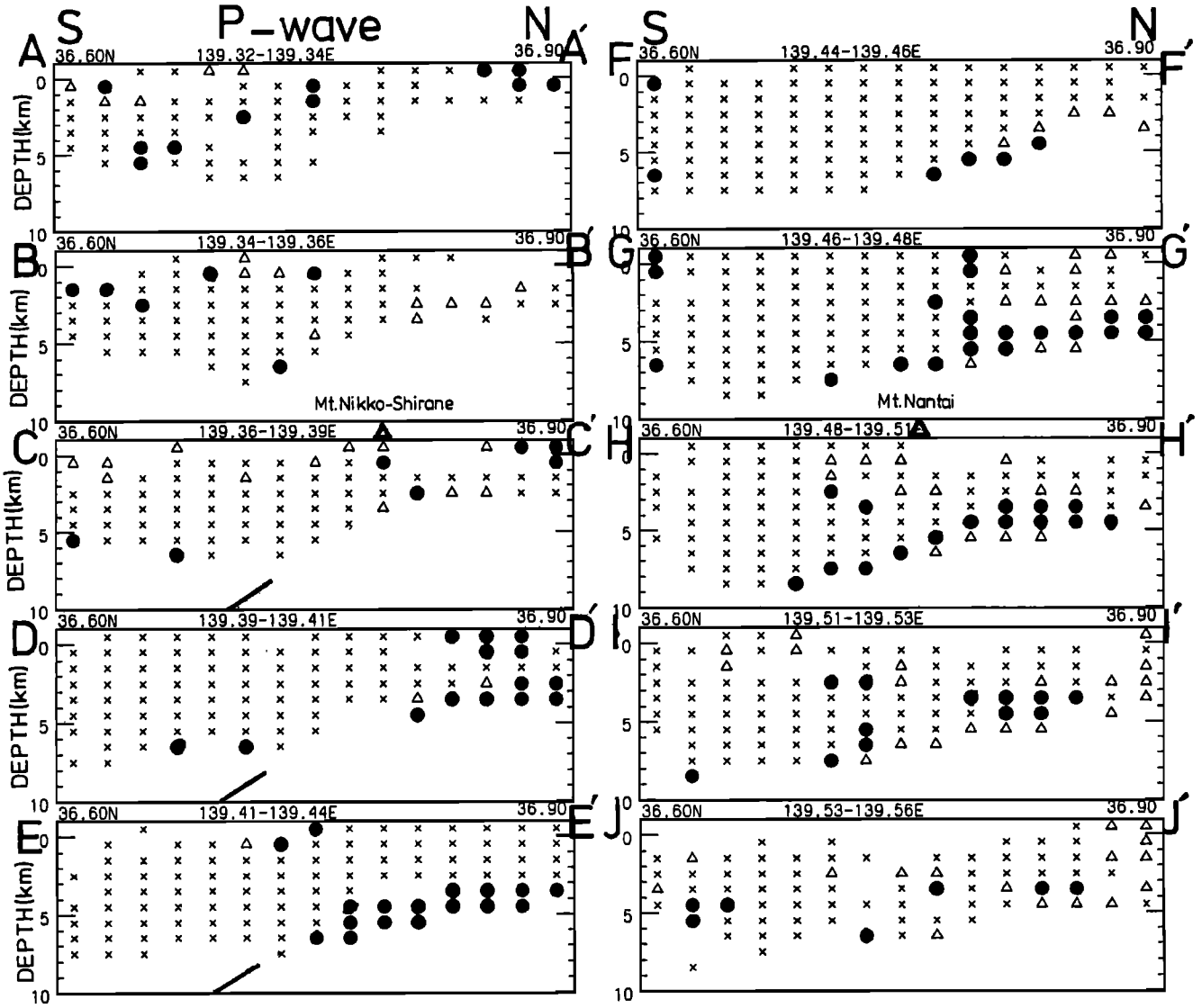

Figure 10. N-S vertical cross sections showing distributions of hot (solid circles), cold (crosses), and uncertain (triangles) blocks estimated from values of the energy ratio for *P* waves. The location of each vertical sections is shown in Figure 9. Solid lines indicate the location of the midcrustal seismic reflector obtained by *Matsumoto and Hasegawa* [1995].

waves become the first arrival in the shadow zone. Since these waves do not propagate through the magma body, their amplitudes are independent on the length of the direct *P* wave ray path in the anomalous zone. The model of the shadow zone can explain the pattern of the energy ratio in Figure 12, which shows a small decrease in the average energy ratio with increase of the hot block numbers. Therefore we consider that an appropriate distribution of hot and cold blocks is obtained by putting both N_c and N_h to be 3.

Seismogram Characteristics for Deep Events

The temporary seismic network, JSO'93 [*Hasegawa*, 1994] also recorded seismograms of regional events occurring along the deep seismic zone below the study area. These data were also used to estimate the deep structure beneath the anomalous zone obtained in the previous section, since no information for the deep structure was obtained from the analysis of shallow events.

Figure 13 shows hypocenters of intermediate depth events used in the present analysis. Since these events occurred far from the temporary network, we used hypocenter parameters, except origin time, determined by the seismic network of Tohoku University. The Tohoku University network collects data from about 80 seismic stations distributed in the wide area from north Kanto to South Hokkaido. Origin times were selected so that the average of *P* wave residuals for the temporary stations were 0.

The result obtained in the preceding section shows

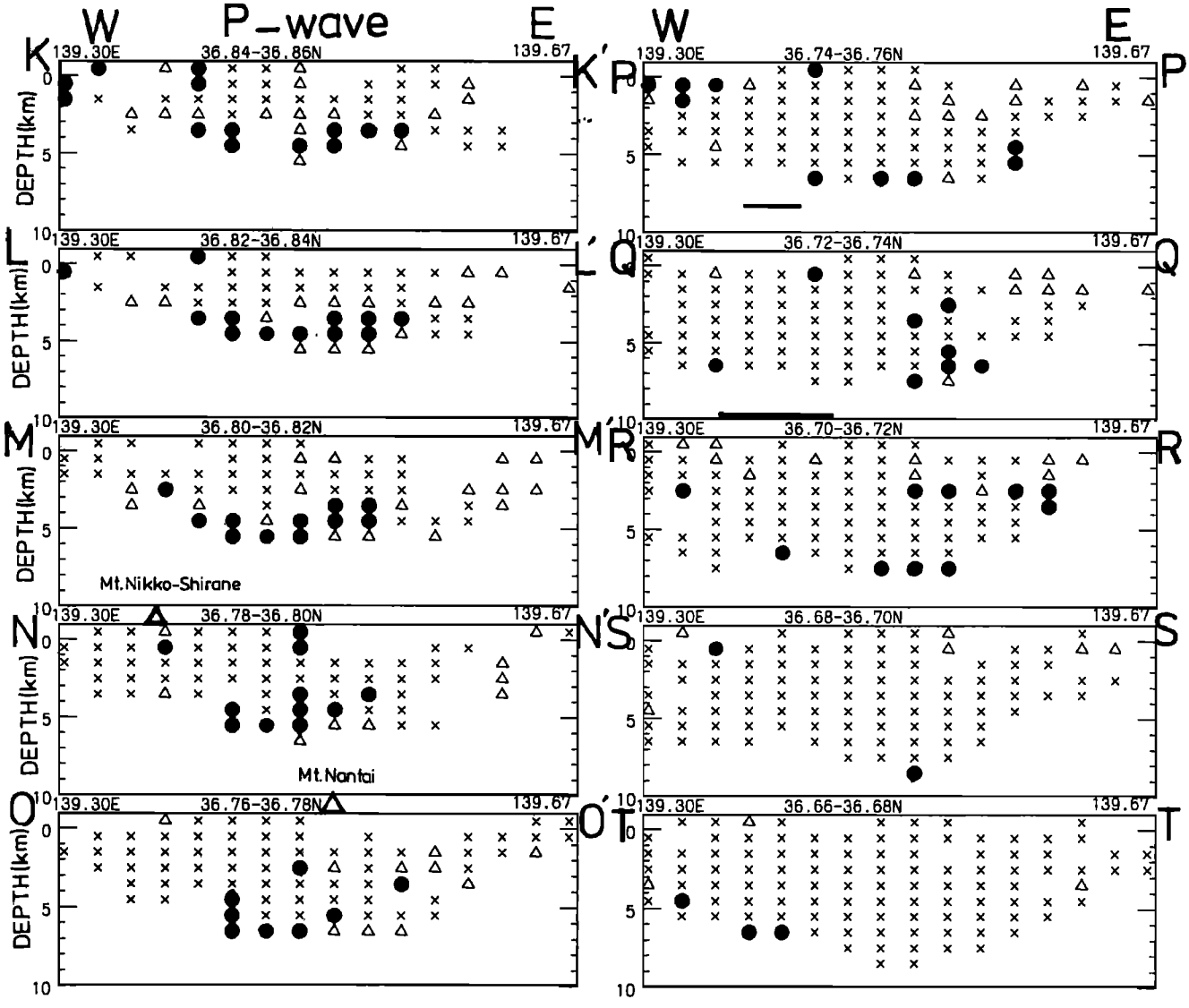

Figure 11. W-E vertical cross sections showing distributions of hot (solid circles), cold (crosses), and uncertain (triangles) blocks estimated from values of the energy ratio for *P* waves. The location of each vertical section is shown in Figure 9. Solid lines indicate the location of the midcrustal seismic reflector estimated by *Matsumoto and Hasegawa* [1996].

the existence of an anomalous zone east of Nikko-Shirane volcano at depths ranging from 3 km to 6 km. As schematically shown in Figure 14, we calculate the horizontal distance(Δ) from the center of the anomalous zone to the ray positions at a 6 km depth. The ray path is calculated by the two-layer velocity model used in the hypocenter location of Tohoku University [*Hasegawa et al.*, 1978]. *P* wave velocity at the surface is 5.4 km/s in the model, and it increases to 7.2 km/s at the upper boundary of the Moho discontinuity which is located at 31 km depth. Seismograms for intermediate depth events shown in Figure 13 are plotted in order of increasing Δ. The center of the anomalous zone is shown by the cross in Figure 9.

Figure 15a shows seismograms with Δ smaller than 5 km. Time axes are shifted so that theoretical arrival times become 2 s. The initial part of the direct *P* wave for these seismograms is obscure and most arrival times are delayed about 0.7 sec. Figure 15b shows seismograms for which Δ is between 5 km and 10 km. A value of the average arrival time delay is about 0.3 s.

Figure 15c shows seismograms with Δ larger than 18 km. The direct *P* waves are clear and there are no arrival time delays in this distance range. The comparison of the seismograms plotted in Figures 15a-15c indicates the existence of the anomalous zone in the same area determined in the preceding section by the analysis of the energy ratio of shallow events.

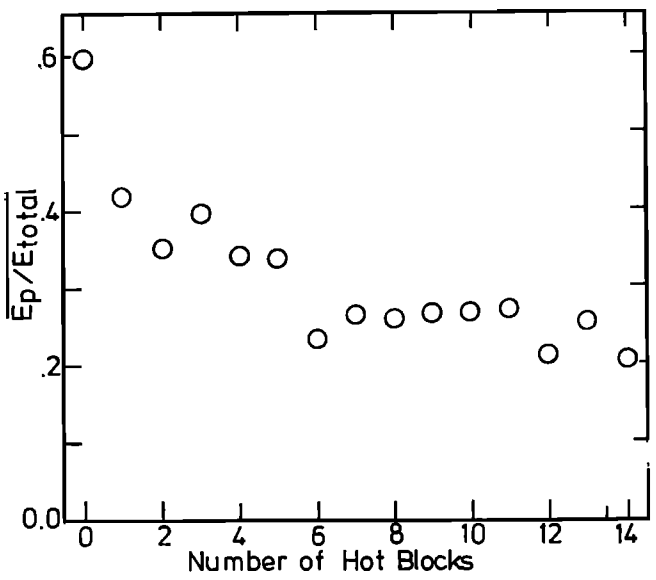

Figure 12. Average energy ratios versus the number of hot blocks, demonstrating the fitness of the obtained model. Average values are calculated by averaging energy ratios of *P* waves for ray paths having the same numbers of hot blocks. There is a remarkable change between average values for zero and one block number, from 0.59 to 0.42. For number of blocks greater than one, the ratio gradually diminishes to 0.2 when number of hot blocks is 14.

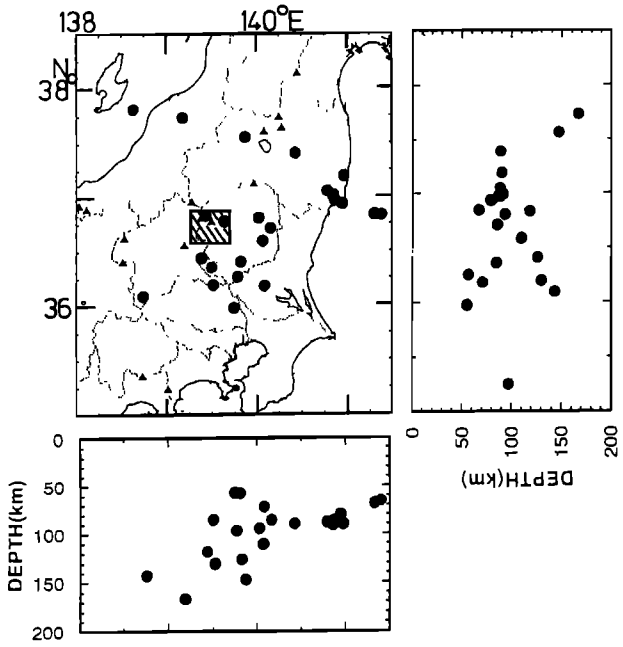

Figure 13. Hypocenter distribution of intermediate depth earthquakes deeper than 50km used in the present analysis. Solid triangles show active volcanoes. The shaded region shows the study area in Figures 9-11.

In order to estimate the approximate location of the bottom of the anomalous zone, we selected seismograms of direct *P* waves which propagate through the deeper part of the anomalous zone. We calculated horizontal distances of ray paths from the center of the anomalous zone at 15 km depth. Seismograms are plotted according to the order of these horizontal distances (Figure 16). As shown in Figure 14, we did not plot seismograms whose ray paths for direct *P* wave cross the shallow part of the anomalous zone; a zone with depths ranging from 4 km to 10 km and with horizontal distances from the center of the anomalous zone less than 7 km. Though there are not many seismograms for small distances, most of their arrival times are delayed by about 0.5 s, suggesting the thickness of anomalous zone to be more than about 10 km.

As mentioned above, *P* wave arrival times are delayed about 0.7 s during propagation into the anomalous zone.

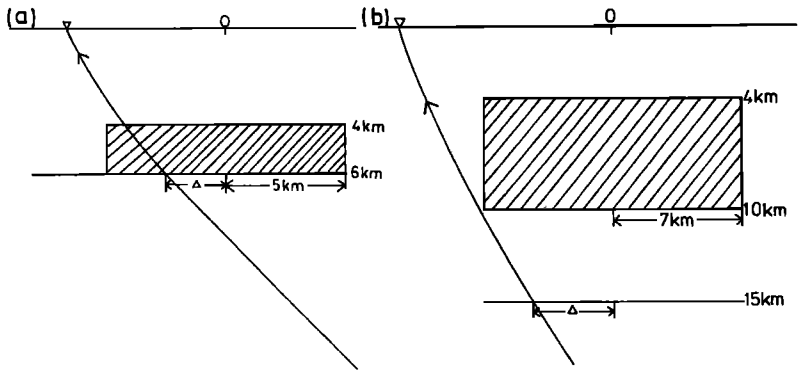

Figure 14. A schematic vertical cross section showing how to measure the distance (Δ) of ray paths at (a) 6 km and (b) 15 km depths from the center of the anomalous zone. The center of the anomalous zone is shown by the plus in Figure 9. The anomalous zone is hatchured, and a ray path of an intermediate depth earthquake is shown by a line. Seismograms crossing through the shaded zone are not included in Figure 16.

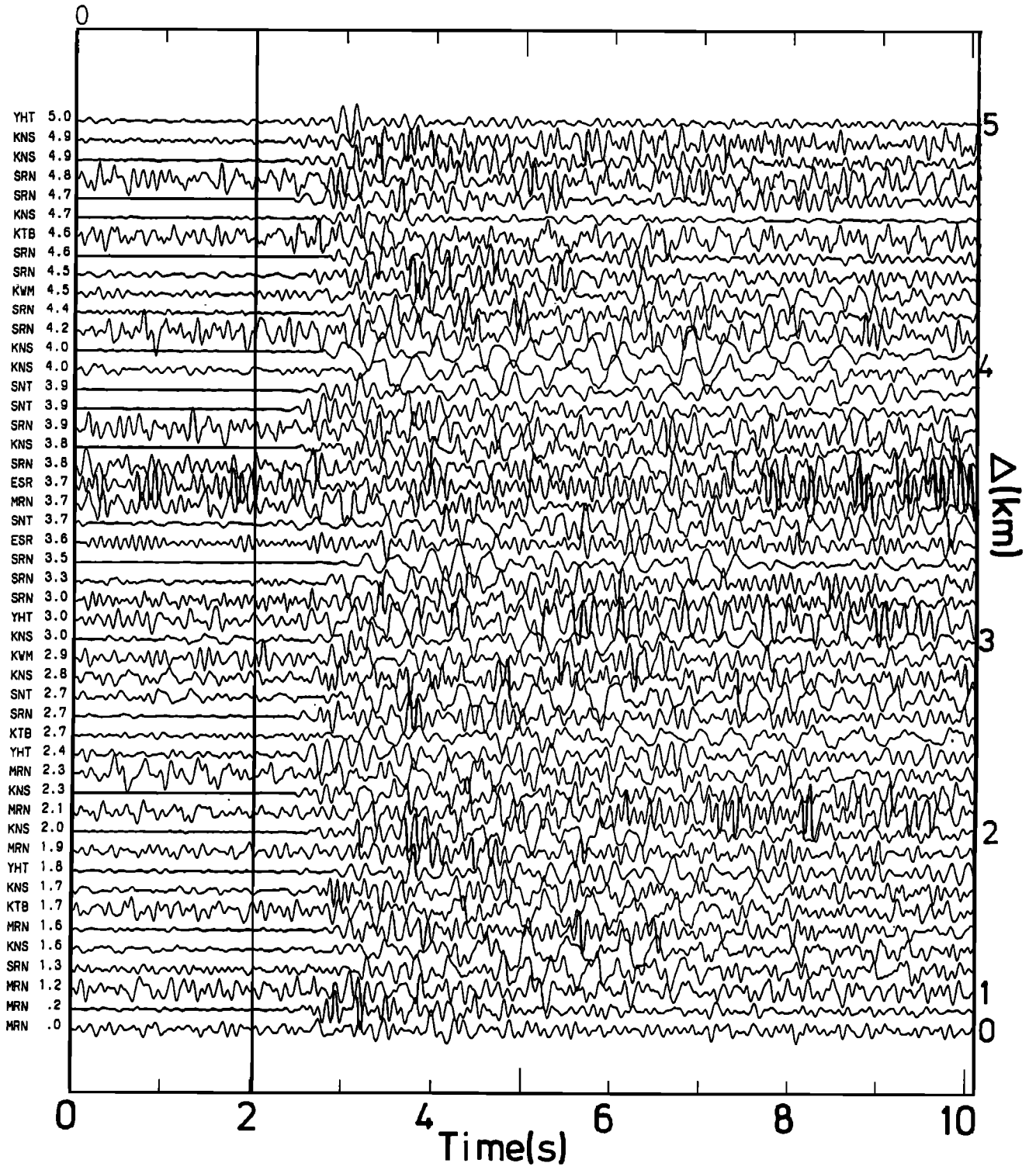

Figure 15a. Plot of seismograms with the ray distance (Δ) at 6 km depth in Figure 14 less than 5 km. Time axes are shifted so that theoretical arrival times of P waves become 2 s. Most of first arrivals for these seismograms are not clear and their arrival times are delayed by about 0.7 s.

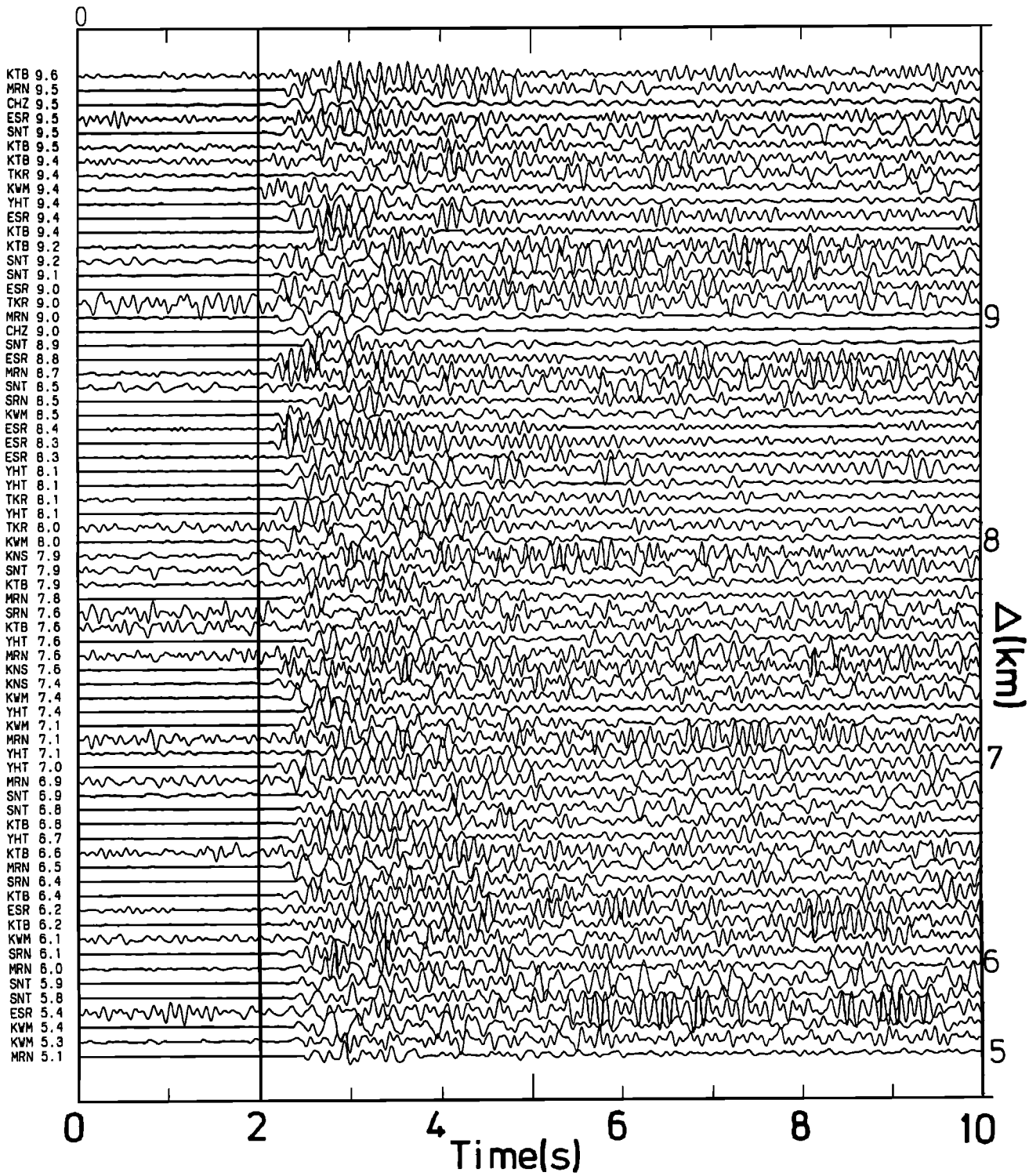

Figure 15b. Plot of seismograms with the ray distance (Δ) at 6 km depth in Figure 14 from 5 km to 10 km. Time axes are shifted so that theoretical arrival times of P waves become 2 s.

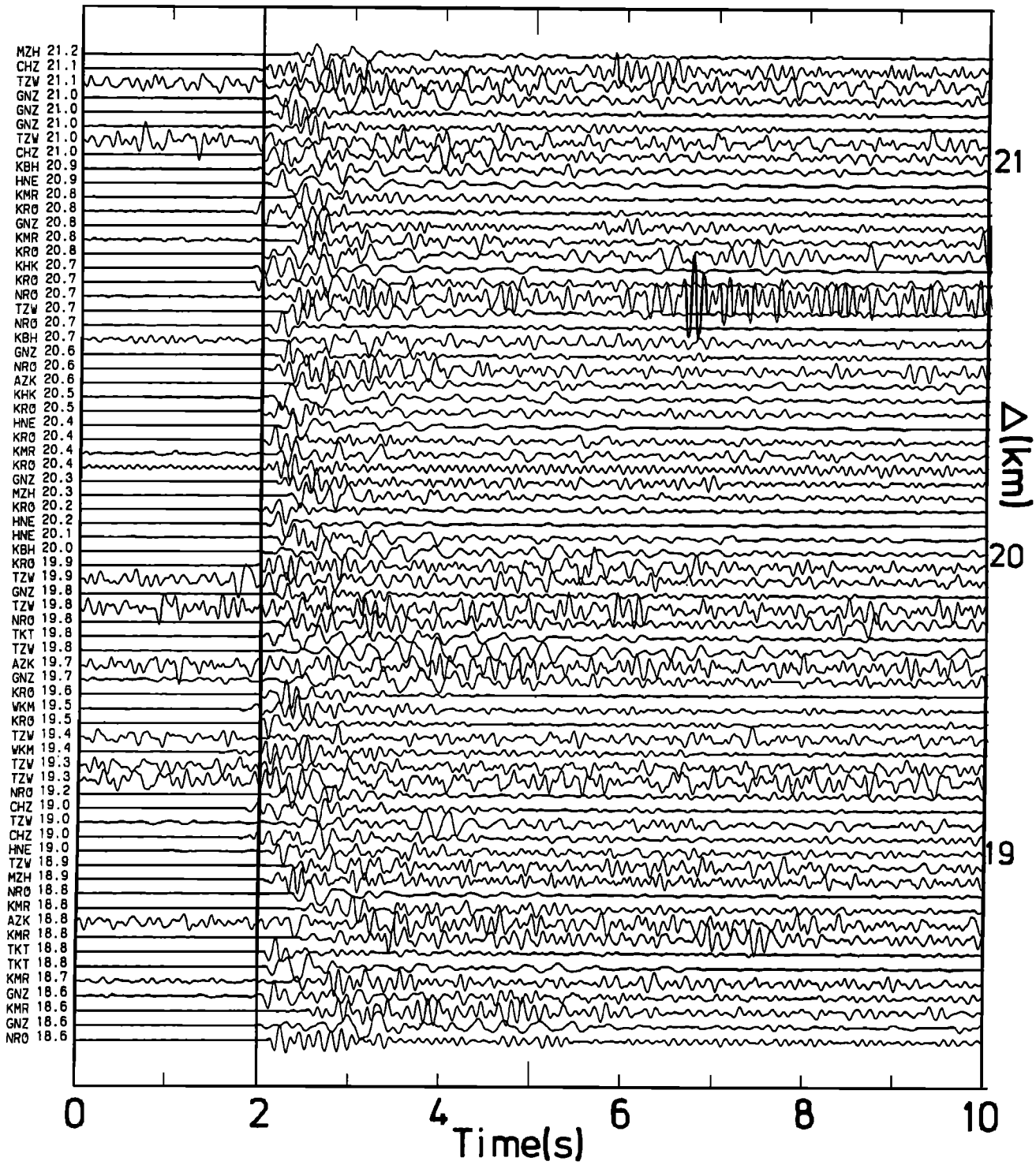

Figure 15c. Plot of seismograms with ray distances(Δ) at 6 km depth in Figure 14 larger than 18 km. Time axes are shifted so that theoretical arrival times of *P* waves become 2 s.

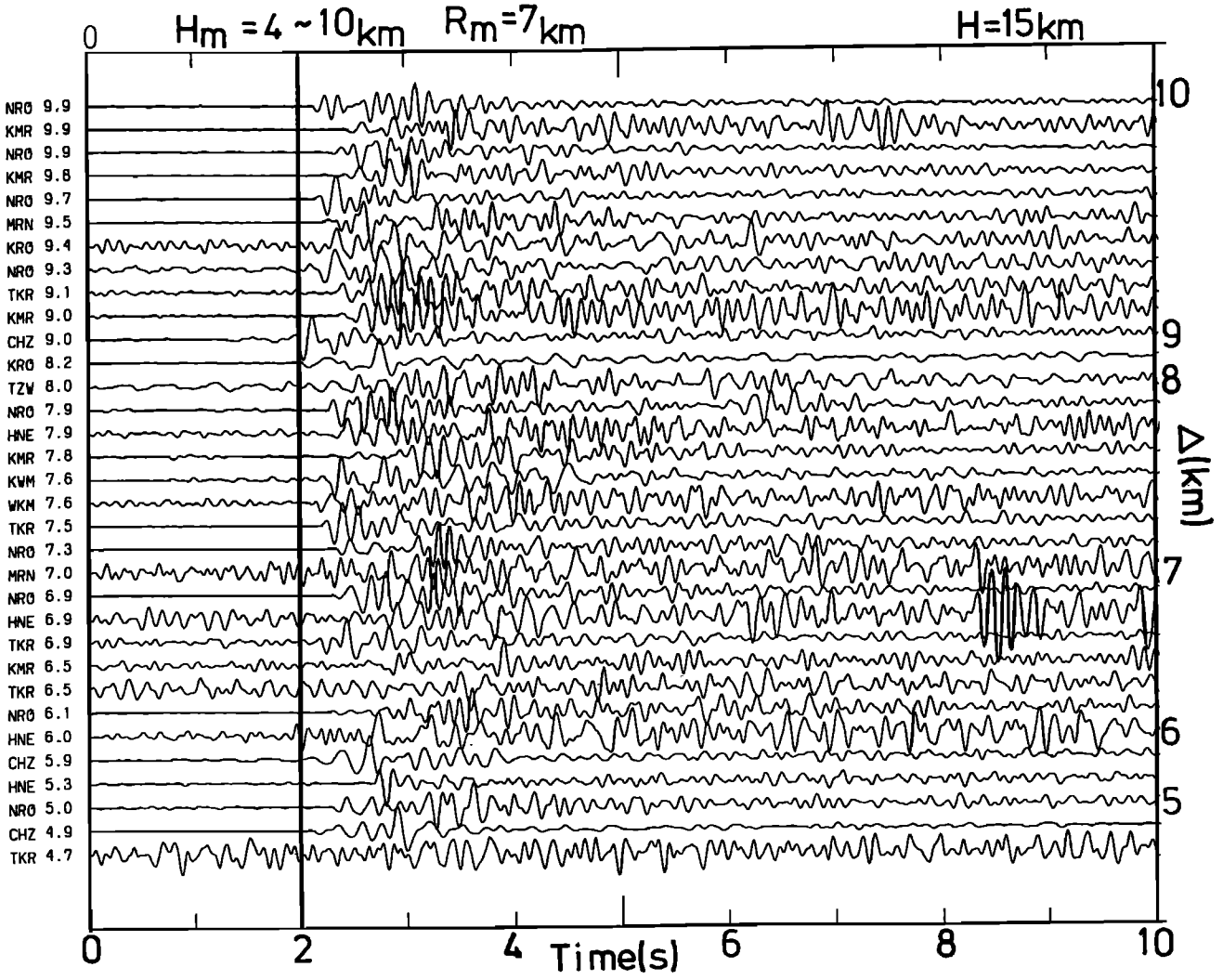

Figure 16. Plot of seismograms according to the order of ray distances(Δ) at 15 km depth in Figure 14. Seismograms are not plotted if they propagate through the shaded zone in Figure 14b, the zone at depths from 4 to 10 km and a diameter of 7 km. Time axes are shifted so that theoretical arrival times become 2 s.

If we assume the first arrival phase to be direct *P* waves, the thickness of the anomalous zone to be 10 km, and the *P* wave velocity to be 6 km/s, the *P* wave velocity in the anomalous zone must be 4.2 km/s, that is, smaller by about 30%. Since the estimated velocity drop is very large, the anomalous zone may be a magma body. Most of the first arrival phases in Figure 15a are very obscure. If they are the diffracted waves, the velocity perturbation in the anomalous zone must be larger than 30%.

Discussion and Conclusions

We have shown that there is an anomalous attenuation zone in the eastern part of Mount Nikko-Shirane volcano. As clear from the shallow event seismograms shown Figure 5, *P* and *S* waves crossing through that zone are highly attenuated. Since it is almost impossible to read arrival times for these seismograms, we can not get arrival time data including information about the seismic velocity in the anomalous zone. Therefore it is very difficult to determine seismic velocity structure in the anomalous zone by the use of arrival time data of shallow events.

It is clear that one can estimate a very detailed shape of a body from the shape of its shadows projected from many directions. If we can know whether or not each observation station is recorded inside or outside the seismic shadow zone from its seismogram, we can image a very precise shape of the anomalous zone, though we can not determine a value of its seismic velocity.

Observed amplitudes of *P* and *S* waves are a function of earthquake size, orientation of the focal mechanism, geometrical spreading, attenuation(Q), and site amplification in the layer just beneath the station. It is very difficult to determine these values precisely by the use of observed short-period seismograms because of the limitation of available station density and the complexity of the velocity and Q structures. For example,

the amplitude of short-period P and S waves depends strongly on the site effect. It was found that observed P wave amplitudes can change by factors of 2-3 times with difference in station locations of only several tens of meters [*e. g.*, *Kaihara et al.*, 1996]. The complexity of the earth structure makes it very difficult to estimate the theoretical amplitude of the short-period seismic waves.

Instead of estimating a theoretical amplitude, we use a new parameter, the energy ratio between the initial part of P or S waves and their coda waves, to discriminate seismograms observed inside or outside the shadow zone. The present study analyzes the energy ratio data for shallow events to image the location of the anomalously low velocity zone and finds that it is at depths greater than 3 km beneath the area east of Nikko-Shirane volcano, which is the only active volcano in this region.

The shallow event result was checked by plotting seismograms for intermediate depth events located in the deep seismic zone. Large arrival time delays were found for ray paths propagating through the anomalous zone. This strongly suggests the effectiveness of the energy ratio method for the imaging of an anomalous zone. The diameter of the anomalously low velocity zone was estimated to be 10 to 15 km. It was found that P wave arrival times are delayed an average of about 0.7 s during the propagation through or around this anomalous zone. If the thickness of the anomalous zone is assumed to be 10 km and observed P waves are direct waves propagating through it, the average arrival time delays require the P wave velocity in the anomalous zone to be smaller by about 30% than that of the surrounding crustal material. Since this value is very large, there may be a magma body in the anomalous zone.

Horiuchi et al. [1988] and *Matsumoto and Hasegawa* [1996] found a distinct seismic reflector in the midcrust, which is considered to be the upper surface of a melted zone, beneath the area south of Nikko-Shirane volcano at depths ranging from 8 to 15 km. *Matsumoto and Hasegawa* [1996] pointed out that the thickness of the reflector body is of the order of 100 m based on a spectral ratio analysis between reflected S and direct S waves. *Matsumoto et al.* [1995] and *Tsumura* [1995] obtained tomographic images of the P and S wave velocity structure and Q structure, respectively, by inverting the JSO'93 data sets for shallow and deep events. They pointed out that there are no low-velocity and low-Q zones beneath the seismic reflector, while their results clearly show the existence of a low-velocity and low-Q zone at the same location as the anomalous zone obtained in the present study. These results suggest that the total volume of the melted zone in and beneath the seismic reflector is much smaller than that in the anomalous zone east of Nikko-Shirane volcano detected by the present study.

As can be seen from Figures 10 and 11, the southwestern boundary of the anomalous zone is very close to the shallower part of the seismic reflector, the distance between them is about 4 km. *Matsumoto and Hasegawa* [1995] found several sheets of seismic reflectors beneath the northern extent of the distinct reflector, though reflected waves from them are not very clear. Their result suggests that the distinct seismic reflector is connected to the anomalous zone found in the present study. Merging these observations together, a vertical cross section in the Nikko-Ashio area is schematically shown in Figure 17, which indicates shapes and locations of the

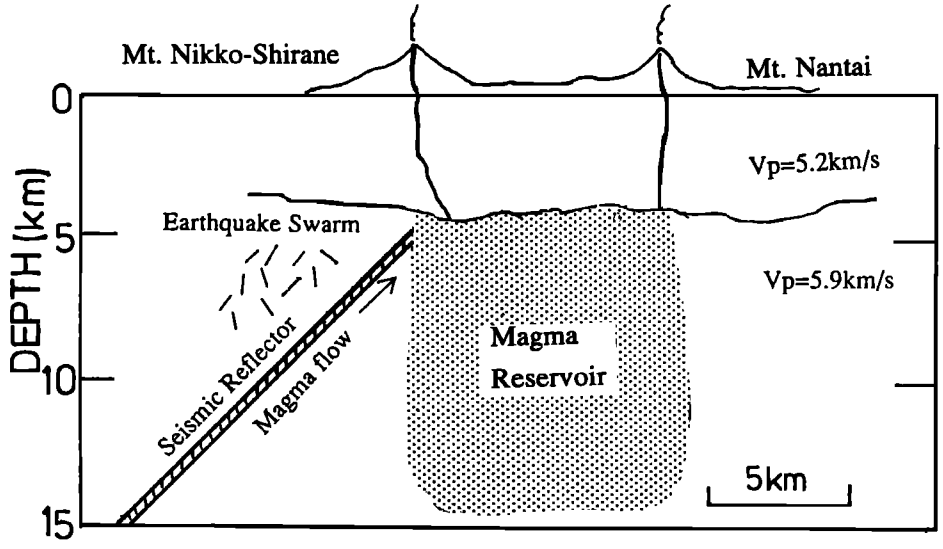

Figure 17. A schematic vertical cross section showing the locations of the seismic reflector, the anomalous zone (magma reservoir), and the earthquake swarm area beneath Nikko-Shirane volcano. Magmas extruded from Nikko-Shirane and Nantai volcanoes were perhaps supplied from the magma reservoir.

seismic reflector and the hypothesized magma reservoir. We suppose that there is a magma reservoir in the lower crust, whose location may be at the deeper extension of the reflector. The magma body from this deep body ascends along the thin steeply dipping conduit to the shallow magma reservoir found in the present study.

Toumiya [1995] calculated time variations in the temperature distribution surrounding and within a very thin magma chamber in the crust. His calculations indicate that about half of the thin magma chamber will be solidified after 20,000 years have passed, if its thickness is about 1 km. This shows that a thin melted zone with thickness of the order of 100 m could not persist for a very long time. However, if there is a magma flow within the reflector body as shown in Figure 17, the thin melted zone may survive, because melted material is being continuously injected before it is solidified.

Matsumoto and Hasegawa [1996] pointed out that there exists seismic reflectors near the upper surface of the anomalous zone found in the present study. However, reflection coefficients for these discontinuities are much smaller than that for the distinct seismic reflector found by *Mizoue et al.* [1982], *Horiuchi et al.* [1988], and *Matsumoto and Hasegawa* [1996]. The present result shows the *P* wave velocity in the anomalous zone to be very low. The small reflectivity at the upper surface of the anomalous zone suggests that the shape of its upper surface is rugged, as shown in Figure 17, or a large velocity gradient exists near the upper surface of the anomalous zone.

Acknowledgments. The authors would like to express their sincere gratitude to the group for the Joint Seismic Observation, who operated the seismic network in and around Nikko Area, Japan. We thank the referees, Allan R. Sanford, Allessandro Amato, and Aldo Zollo, for their constructive criticisms.

References

Ake, J. P., and A. R. Sanford, New evidence for the existence and internal structure of a thin layer of magma at mid-crustal depths near Socorro, New Mexico, *Bull. Seismol. Soc. Am., 78*, 1335-1359, 1988.

Brown, L. D., C. E. Chapin, A. R. Sanford, S. Kaufman, and J. Oliver, Deep structure of the Rio Grande Rift from seismic reflection profiling, *J. Geophys. Res, 85*, 4773-4800, 1980.

Catchings, R. D., Crustal structure of east central Oregon: Relation between Newberry Volcano and regional crustal structure, *J. Geophys. Res., 93*, 10,081-10,094, 1988.

Chiarabba, C., A. Amato, and A. Fiordelisi, Upper crustal tomographic images of the Amiata-Vulsini geothermal region, central Italy, *J. Geophys. Res., 100*, 4053-4066, 1995.

Dawson, P. B., J. R. Evans, and H. M. Lyer, Teleseismic tomography of the compressional wave velocity structure beneath the Long Valley region, California, *J. Geophys. Res., 95*, 11,021-11,050, 1990.

Group for the 1993 Joint Seismic Observation, A very dense seismic array observation for imaging the crust and seismic sources--The 1993 Joint Seismic Observation in and around Nikko area, paper presented at the 1994 Japan Earth and Planetary Science Joint meeting, Sponsored by 13 societies about Earth and Planetary Science, Sendai, 1994.

Hasegawa, A., 1993 Joint Seismic Observation in and around Nikko area (in Japanese), *Earth Mon., 16*(4), 200-207, 1994.

Hasegawa, A., N. Umino, and A.Takagi, Double-planed structure of the deep seismic zone in the northeastern Japan arc, *Tectonophysics, 47*, 43-58, 1978.

Hasegawa, A., D. Zhao, S. Hori, A. Yamamoto and S. Horiuchi, Deep structure of the northeastern Japan arc and its relationship to seismic and volcanic activity, *Nature, 352*(6337), 683-689, 1991.

Hasemi, A., H. Ishii, and A. Hasegawa, Fine structure beneath the Tohoku District, northeastern Japan arc, as derived by an inversion of *P*-wave arrival times from local earthquakes, *Tectonophysics, 101*, 245-265, 1984.

Hori, S., and A. Hasegawa, Location of a mid-crustal magma body beneath Mount Moriyoshi, northern Akita Prefecture, as estimated from reflected SxS phase (in Japanese with English abstract), *J. Seismol. Soc. Jpn., 44*, 39-48, 1991.

Horiuchi, S. H., Ishii, and A. Takagi, two-dimensional depth structure of the crust beneath the Tohoku District, the north-eastern Japan arc, 1, Method and Conrad discontinuity, *J. Phys. Earth, 30*, 255-281, 1982.

Horiuchi, S., A. Hasegawa, A. Takagi, A. Ito, M. Suzuki, and H. Kameyama, Mapping of a melting zone near Mount Nikko-Shirane in northern Kanto, Japan, as inferred from *SxP* and *SxS* reflections, *Tohoku Geophys. J., 31*, 43-55, 1988.

Horiuchi, S., et al., Location of magma reservoir beneath Bandai Volcano deduced from fan-shooting seismic survey(in Japanese with English abstract), *J. Seismol. Soc. Jpn., 43*, 379-387, 1990.

Horiuchi, S., T. Matsuzawa, and A. Hasegawa, A real-time processing system of seismic wave using personal computers, *J. Phys. Earth, 40*, 395-406, 1992.

Inamori, T., S. Horiuchi, and A. Hasegawa, Location of mid-crustal reflectors by a reflection method using aftershock waveform data in the focal region of the

1984 western Nagano Prefecture earthquake, *J. Phys. Earth, 40,* 379-393, 1992.

Ito, A., Y. Haryu, M. Suzuki, T. Matsumoto, A. Hasegawa, and M. Kasahara, Seismic activity in the Nikko-Ashio region before and after the 1993 Nikko Joint Observation(in Japanese), *Earth Mon.*, *17*(2), 76-80, 1995.

Iwase, R., S. Urabe, K. Katsumata, M. Moriya, I. Nakamura, and M. Mizoue, Mid-crustal magma body in southwestern Fukashima Prefecture detected by reflected waves from microearthquakes, *Programme Abstr. Seismol. Soc. Jpn.*, no. 1, 185, 1989.

Kaihara, K, S. Horiuchi, A. Hasegawa, K. Nida, T. Kono, S. Hori, and K. Kasahara, Spatial variation of high frequency seismic waves caused by a lateral heterogeneity of sedimentary layer (in Japanese with English Abstract), *J. Seismol. Soc. Jpn.*, *49*, 169-177, 1996.

Lees, J. M., and R. S. Crosson, Tomographic inversion for three-dimensional velocity structure at Mount St. Helens using earthquake data, *J. Geophys. Res.*, *94*, 5716-5728, 1989.

Matsumoto, S., and A. Hasegawa, Distribution of S-wave reflector in the Nikko-Ashio area(in Japanese), *Earth Mon.*, *17*(2), 85-89, 1995.

Matsumoto, S., and A. Hasegawa, Distinct *S* wave reflector in the midcrust beneath Nikko-Shirane volcano in the northeastern Japan arc, *J. Geophys. Res.*, *101*, 3067-3083,1996.

Matsumoto, S., T. Tsumura, T. Okada, and A. Hasegawa, *P* wave velocity structure beneath Nikko area (in Japanese), *Earth Mon.*, *17*(2), 81-85, 1995.

Mizoue, M., and Y. Ishiketa, Detection of melting zone beneath the focal area of the 1984 western Nagano Prefecture earthquake and beneath the southern foot of Mount Ontake (in Japanese), *Earth Mon*, *10*(11), 700-705, 1988.

Mizoue, M., I. Nakamura, and T. Yokota, Mapping of an unusual crustal discontinuity by microearthquake reflection in the earthquake swarm area near Ashio, northwestern part of Tochigi Prefecture, central Japan, *Bull. Earthquake. Res. Inst. Univ. Tokyo, 57*, 653-686, 1982.

Murase, T., and T. Suzuki, Ultrasonic velocity of longitudinal waves in molten rocks, *J. Fac. Sci. Hokkaido Univ., Ser. VII*, *2*(3), 273-285, 1966.

Nishiwaki, M., Y. Morita, S. Ryu, T. Kakishita, Y. Osada, and N. Nagai, Location of anomalous reflectors, as determined from SxS phases observed by array network of Matsushiro, *Programme Abst. Seismol. Soc. Jpn.*, no.1, 184, 1989.

Obara, K., A. Hasegawa, and A. Takagi, Three dimensional *P* and *S* wave velocity structure beneath the northeastern Japan arc (in Japanese with English Abstract), *J. Seismol. Soc. Jpn.*, *39*, 201-215, 1986.

Ogino, I., Seismic activity in Ashio area, Tochigi Prefecture, preliminary report(in Japanese), *Bull. Earthquake. Res. Inst. Univ. Tokyo, 12*, 159-169, 1974.

Ono, K., K. Ito, I. Hasegawa, K. Ichikawa, S. Iizuka, T. Kurata, and H. Suzuki, Explosion seismic studies in south Kyushu especially around Sakurajima Volcano, *J. Phys. Earth, 26*, s309-s319, 1978.

Romero, A. E. Jr., T. V. McEvilly, and E. L. Majer, Velocity structure of the Long Valley caldera from the inversion of local earthquake *P* and *S* travel times, *J. Geophys. Res.*, *98*, 19,869-19,879, 1993.

Sanford, A. R., O. Alptekin, and T. R. Toppozada, Use of reflection phases on microearthquake seismograms to map an unusual discontinuity beneath the Rio Grande Rift, *Bull. Seismol. Soc. Am., 63*, 2021-2034, 1973.

Toumiya, A., A magma-feeding system and its thermal effect on seismicity at Mount Nikko-Shirane(in Japanese), *Earth Mon*, 17(2), 107-112, 1995.

Tsumura, N., Simultaneous estimation of attenuation structure, source parameters and site response spectra--Application to the northeastern part of Honshu, Japan, Doctor's thesis, Tohoku Univ., Sendai, Japan, 1995.

Yamamoto, K., M. Kosuga, and T. Hirasawa, A theoretical method for determination of effective elastic constants of isotropic composites, *Tohoku Geophys J.*, *28*(1) 47-67, 1981.

Zhao, D., A. Hasegawa, and S. Horiuchi, Tomographic imaging of *P* and *S* wave velocity structure beneath northeastern Japan, *J. Geophys. Res, 97*, 19,909-19,928, 1992.

Zhao, D., A. Hasegawa, and H. Kanamori, Deep structure of Japan subduction zone as derived from local, regional, and teleseismic events, *J. Geophys. Res.*, *99*, 22,313-22329, 1994.

A. Hasegawa and S. Horiuchi, Research Center for Prediction of Earthquakes and Volcanic Eruptions, Faculty of Science, Tohoku University, Sendai 980-77 Japan. (email: hasegawa@aob.geophys. tohoku.ac.jp, horiuchi@aob.geophys.tohoku.ac.jp).

N. Tsumura, Department of Earth Science, Faculty of Science, Chiba University, Chiba, 263, Japan. (email:tsumura@earth.s.chiba-u.ac.jp)

(Received May 17, 1996; revised March 20, 1997; accepted March 31, 1997.)